

# Gold nanoparticle-based fluorescence quenching via metal coordination for assaying protease activity

Se Yeon Park · So Min Lee · Gae Baik Kim · Young-Pil Kim

Published online: 25 October 2012

© The Author(s) 2012. This article is published with open access at SpringerLink.com

**Abstract** We report a gold nanoparticle (AuNP)-based fluorescence quenching system via metal coordination for the simple assay of protease activity. Carboxy AuNPs (5 nm in core diameter) functioned as both quenchers and metal chelators without requiring further modification with multidentate ligands; therefore, they were strongly associated with the hexahistidine regions of dye-tethered peptides in the presence of Ni(II) ions, leading to notable fluorescence quenching over the varying molar ratios of dye to AuNP. Upon the addition of matrix metalloproteinase-7 (MMP-7), the fluorescent intensity was efficiently recovered in one-pot mixture especially at 10:1–100:1 molar ratios of dye to AuNP. Consequently, the dequenching degree was dependent on the MMP-7 concentration in a hyperbolic manner, ranging from as low as 10 to 1,000 ngmL<sup>-1</sup>. In this regard, we anticipate that the developed system will give us a general way to construct nanoparticle–dye conjugates and will find applications in the analyses of many other proteases mediating significant biological processes with low background and high sensitivity.

**Keywords** Gold nanoparticle · Quenching · Metal coordination · Protease · Matrix metalloproteinase

## Introduction

The interactions between gold nanoparticles (AuNP) and organic dyes have gained considerable interest in biochemical assay because they provide many advantages regarding quenching efficiency and photostability over the classical dye quencher system [1–6]. The ability of AuNPs to induce fluorescence quenching of proximal dyes is reported to be directed by a surface energy transfer process [7–9]; the rate of energy transfer from a dye to AuNP depends on the inverse of fourth power of the donor–acceptor separation, which triggers a much longer working distance (up to 22 nm) than that observed in a traditional fluorescence resonance energy transfer system (up to 10 nm, due to the inverse sixth power distance dependency). To this end, AuNP–organic dye couples have been implemented for the highly sensitive detection of oligonucleotides [10–12], proteins [13–17], and other small molecules [18–20].

Recently, the activities of enzymes such as proteases and nucleases have also been analyzed using activatable “switch-on” fluorescent nanoprobe in order to gain some insight into enzyme kinetics or biological activity [21–23]. In particular, proteases have been recognized as important targets due to their roles that are involved in multiple processes during malignant progression, including tumor angiogenesis, invasion, and metastasis [24, 25]. Protease-detecting methods, therefore, have been accomplished by incorporating relatively stable peptides between the AuNP and the dye via either biotin–avidin interaction [22, 26] or thiol-mediated coupling [27–29]. In addition to these conjugations, nickel–nitrilotriacetic acid (Ni(II)–NTA)-modified AuNPs were recently demonstrated by several groups [30, 31] since Ni(II)–NTA provides high binding

Se Yeon Park, So Min Lee and Gae Baik Kim contributed equally to this work.

S. Y. Park  
Department of Chemical Engineering, Hanyang University,  
Seoul 133-791, South Korea

S. M. Lee  
Department of Bio Engineering, Hanyang University,  
Seoul 133-791, South Korea

G. B. Kim · Y.-P. Kim (✉)  
Department of Life Science, Hanyang University,  
Seoul 133-791, South Korea  
e-mail: ypilkim@hanyang.ac.kr

G. B. Kim · Y.-P. Kim  
Research Institute for Natural Sciences, Hanyang University,  
Seoul 133-791, South Korea

affinity ( $K_d=10^{-13}$ M) for a hexahistidine tag at pH 8.0 [32], which has been widely used as one of the most useful affinity methods. However, these Ni affinity nanoconjugates have been only limited to capture or label proteins with polyhistidine tags, and there was little attempt for enzyme activity study. As an alternative, to enable an easy surface modification based on Ni affinity, Rao's group reported that NTA-free carboxy quantum dot (QD) could be conjugated to his-tagged luciferases in the presence of nickel ions, which developed a QD–bioluminescence resonance energy transfer system to assay protease activity [33]. On the basis of this observation, we envisioned that the use of his-tag-containing peptide affinity tag would allow a site-specific and multivalent conjugation to carboxy AuNPs and would generate a shorter distance between the AuNP and the organic dye, which is favorable for higher energy transfer efficiency regime than that of the biotin–avidin strategy.

Here, we demonstrate a simple fluorescence quenching system using carboxy AuNPs and dye-conjugated peptides and its application to protease assay. A facile conjugation of a dye-coupled peptide to the carboxy AuNP was made possible in the presence of Ni; the resultant AuNP–dye conjugate via metal affinity was used for the detection of matrix metalloproteinase (MMP) activity. We chose MMP as a model protease because MMPs play a crucial role in a wide variety of processes including tumor metastasis, inflammation, growth differentiation, and cell signaling [34–36]. To achieve the optimal fluorescence quenching and dequenching system by protease activity, the quenching efficiency and protease-induced recovery yield of AuNPs toward an organic dye (5(6)-carboxytetramethylrhodamine, TAMRA) was compared in terms of the dye-to-AuNP ratio. Details are reported herein.

## Experimental section

### Materials

Nickel(II) chloride hexahydrate (99.9 %,  $\text{NiCl}_2 \cdot 6\text{H}_2\text{O}$ ), hydrogen tetrachloroaurate(III) trihydrate (99.9 %  $\text{HAuCl}_4 \cdot 3\text{H}_2\text{O}$ ), sodium citrate dihydrate (trisodium salt,  $\text{C}_6\text{H}_5\text{Na}_3\text{O}_7 \cdot 2\text{H}_2\text{O}$ ), and sodium borohydride (99 %,  $\text{NaBH}_4$ ) were purchased from Sigma-Aldrich. Carboxy-PEG<sub>12</sub>-thiol and methyl-PEG<sub>4</sub>-thiol were purchased from Thermo Scientific. Active matrix metalloproteinase-7 (MMP-7) enzyme was purchased from Merck4Biosciences. The TAMRA-labeled peptide (TAMRA-GPLGMRGLHHHHH) was synthesized from Pepton, Inc. (Korea). All chemicals were of analytical grade and were used as received.

### Synthesis of AuNPs

AuNPs were synthesized by reduction and stabilization with citrate. Briefly, 100  $\mu\text{L}$  of a stock solution containing 300 mM of  $\text{HAuCl}_4 \cdot 3\text{H}_2\text{O}$  was added to 100 mL of distilled water to give a final concentration of 300  $\mu\text{M}$  followed by vigorous stirring. To this solution, 2 mL of 30 mM sodium citrate dihydrate was added at a final concentration of 600  $\mu\text{M}$  (the molar ratio of tetrachloroaurate to sodium citrate is 1:2) and stirred. For the fast reduction and formation of gold colloids, 100  $\mu\text{L}$  of a stock solution containing 300 mM of  $\text{NaBH}_4$  was quickly added to the reaction solution followed by stirring. The clustering of AuNPs was checked by UV–Visible spectroscopy (Cary 60 UV–Vis, Agilent Technologies), and the average size of AuNPs was estimated to be  $5.1 \pm 1.4$  nm ( $n=100$ ) using a field emission transmission electron microscope (FE-TEM; FEI Tecnai G2F30S-TWIN, the Netherlands). Surface modification of the synthesized AuNPs was performed with the 1:1 mixture of methyl-PEG<sub>4</sub>-thiol and carboxy-PEG<sub>12</sub>-thiol (total, 100  $\mu\text{M}$ ), which was added to the citrate-stabilized AuNP solution (final, 50 nM). Since the used 5-nm AuNP is estimated to have 3,858 Au atoms in total and 984 Au atoms at its surface based on the reported calculation method [37, 38], the 2,000:1 ligand-to-AuNP molar ratio was used to ensure the complete surface modification of AuNPs. After 2 h of incubation under convection, the carboxy-modified AuNPs were purified using an Amicon® Ultra Centrifugal Filter Unit (50 kDa, MWCO) and centrifugation (8,000 $\times g$  for 10 min). The final concentration of the AuNPs in solution was calculated using the molar extinction coefficient ( $1.2 \times 10^7 \text{M}^{-1} \text{cm}^{-1}$ ) at 520 nm.

### Analysis of fluorescence quenching

For quenching experiments, the TAMRA peptide (2.5  $\mu\text{L}$  at 10  $\mu\text{M}$ ) was mixed with varying amounts of carboxy AuNPs (2.5–25  $\mu\text{L}$  at 1  $\mu\text{M}$ ) at a 100:1–1:1 ratio of the TAMRA peptide and AuNP in the absence or presence of  $\text{NiCl}_2$  (10  $\mu\text{L}$  at 1 mM). All reactions were performed at a final volume of 100  $\mu\text{L}$  in 20 mM Tris buffer (pH 7.5) at RT. After 30 min of incubation, the fluorescence spectra were measured at an excitation wavelength of 550 nm using a spectrofluorometer (FS-2, Sinco, South Korea). We initially tested the self-quenching and detection range of the TAMRA-conjugated peptide. Self-quenching was significant at more than 10  $\mu\text{M}$  TAMRA; therefore, the final concentration of the TAMRA-conjugated peptide in this study was determined to be 250 nM.

### Protease assay

In a one-pot method, AuNPs (2.5 or 5  $\mu\text{L}$  at 1  $\mu\text{M}$ ), TAMRA peptide (2.5  $\mu\text{L}$  at 10  $\mu\text{M}$ ),  $\text{NiCl}_2$  (10  $\mu\text{L}$  at

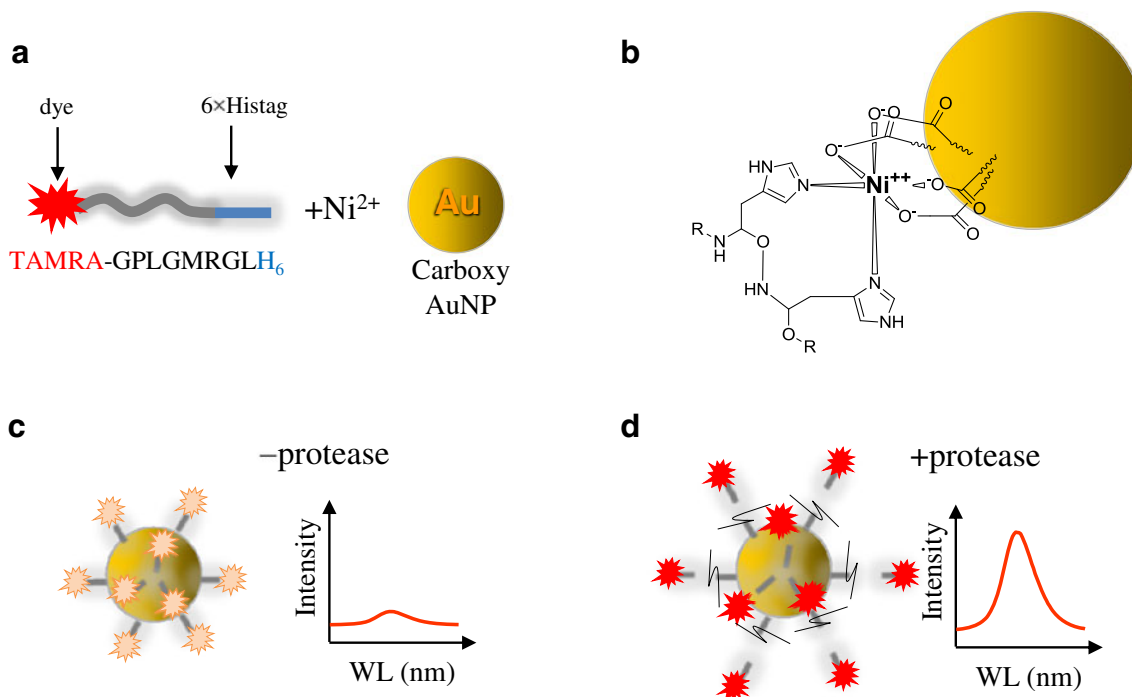
1 mM), and MMP-7 protease (10  $\mu$ L at different stock concentrations) were mixed at a time in 20 mM Tris buffer (pH 7.5) to give a final volume of 100  $\mu$ L and incubated at 37  $^{\circ}$ C for 2 h. It was followed by monitoring the emission spectra of the solution using a spectrofluorometer. In a two-step method, TAMRA peptide (2.5  $\mu$ L at 10  $\mu$ M), MMP-7 (10  $\mu$ L at different stock concentrations), and 20 mM Tris buffer (77.5  $\mu$ L) were initially mixed and incubated at 37  $^{\circ}$ C for 2 h, followed by the addition of AuNPs (2.5 or 5  $\mu$ L at 1  $\mu$ M) and NiCl<sub>2</sub> (10  $\mu$ L at 1 mM). After additional incubation at room temperature for 30 min, the AuNP mixture was subjected to fluorescence scanning. Fluorescence intensity was normalized to the background intensity from the control solution without protease.

## Results and discussion

To construct an efficient quenching system, peptide substrates comprising red dyes (TAMRA) at their N-termini and hexahistidines at their C-termini were mixed with carboxy AuNPs in the presence of Ni(II) ions (Scheme 1a). As a consequence, a dye-to-AuNP quenching was induced by a strong association between polyhistidine residues of the TAMRA peptide and the carboxy groups of the AuNPs via the coordination of Ni(II) metal ions (electron pair acceptors; Scheme 1b). Although common metal-chelating agents

including NTA, iminodiacetic acid (IDA), carboxymethylated aspartic acid, and tris(carboxymethyl)ethylenediamine are available and being widely used for binding polyhistidine tag [39], the chelator-free metal affinity here can be achieved by only the surface-exposed carboxyl groups on the AuNPs. Since highly compacted carboxyl groups in the nanostructured surface can function like multidentate chelators, the binding affinity of Ni(II)-his-tagged carboxy AuNP is likely to be comparable to that of chelator-mediated conjugation (e.g., Ni(II)-his-tagged NTA; our unpublished data), which allowed for the higher quenching efficiency of the dye to AuNP due to their close proximity. In addition, site-specific conjugation and the simplicity of Ni(II)-his-tagged carboxy AuNP were further advantageous for protease assay. Based on this conjugation principle, fluorescence quenching and dequenching were strongly induced in the absence and the presence of protease, respectively (Scheme 1c, d).

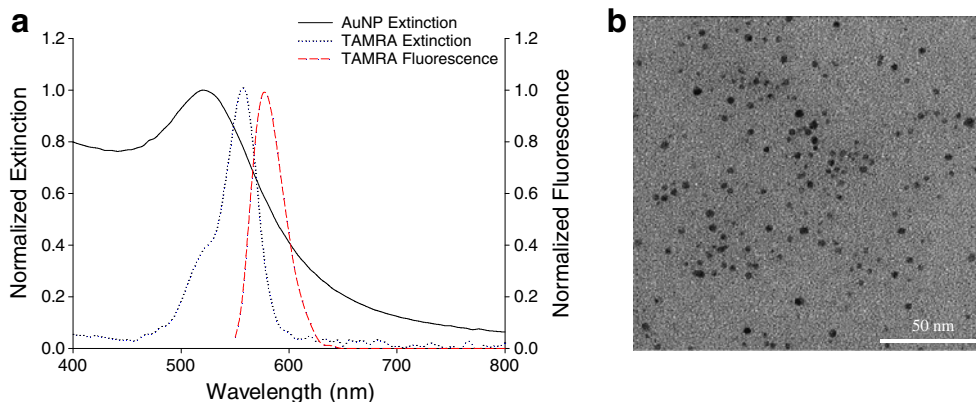
The carboxy AuNPs were synthesized from citrate-stabilized AuNPs by conjugating carboxy-PEG-thiol and were characterized using a UV–Vis spectrophotometer and FE-TEM, which represented a strong surface plasmon resonance band near 520 nm and around 5 nm in diameter (Fig. 1). The extinction and fluorescent emission spectra of the TAMRA dye were also displayed in Fig. 1a. To check the quenching efficiency of the AuNP, different concentrations of the carboxy AuNPs, while maintaining the concentration of the



**Scheme 1** **a** Schematic representation of the component of the AuNP–dye conjugate for protease assay. **b** Schematic of the coordination of the Ni(II) ion with the histidines of peptides and the carboxyl groups on

the AuNP. **c** Resultant fluorescence quenching. **d** Dequenching of the dye-conjugated AuNPs illustrated in the absence and the presence of protease

**Fig. 1** **a** Normalized extinction spectra of AuNPs (black solid) and the TAMRA dye (black dotted) and emission spectrum for the TAMRA dye (red dashed) showing considerable overlap of AuNP extinction and TAMRA emission. **b** High-resolution TEM image of carboxy AuNPs with a diameter of  $5.1 \pm 1.4$  nm ( $n=100$ )



TAMRA peptide constant, were added to the TAMRA peptide (TAMRA-GPLGMRGLH<sub>6</sub>) in the absence or the presence of Ni. As shown in Fig. 2a, the fluorescence intensity declined as the TAMRA-to-AuNP molar ratio decreased from 100:1 to 1:1 even in the absence of Ni. Since the amount of TAMRA was fixed at varied concentrations of AuNPs, the changes in fluorescence intensity were attributed to a quenching effect by the AuNPs. However, this result is probably due to a dynamic collisional quenching effect rather than an affinity-induced

one because Ni-free TAMRA peptide can also be adsorbed on the AuNP by a diffusion-driven electrostatic interaction. In contrast, the addition of Ni facilitated a strong quenching effect by the proximate conjugation between the AuNP and dye, leading to a relatively large decrease in fluorescence intensity over all molar ratios (Fig. 2b). It was shown in Fig. 2c that the Ni(II) ion induced very effective quenching between the TAMRA peptide (His<sub>6</sub>) and the carboxy AuNP (Fig. 2c) compared to the TAMRA dye without AuNPs.

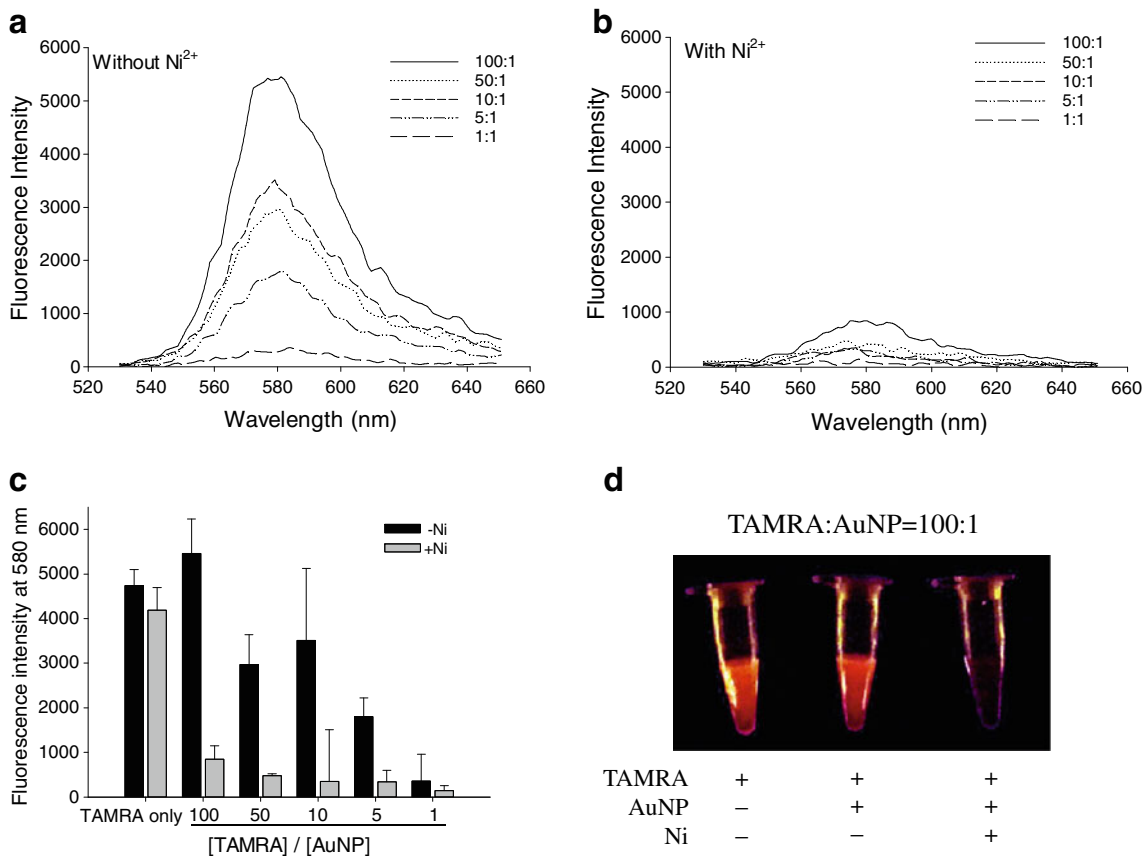


**Fig. 2** Fluorescence spectra of the TAMRA peptide at different concentrations of AuNPs in the absence (a) or the presence (b) of Ni. The molar ratios of TAMRA to AuNP were varied from 100:1 to 1:1 (from top to bottom). c Maximal fluorescence intensities at 580 nm from (b)

and (c) were compared as bar graphs in the absence or the presence of Ni. d Fluorescent images of the TAMRA peptide with and without AuNP or Ni

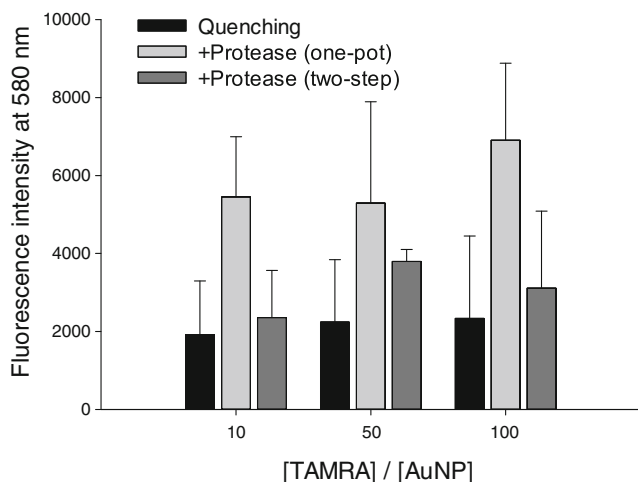


**Fig. 3** Changes in the fluorescence intensities of the AuNP-quenched TAMRA conjugate before and after enzyme reaction at different molar ratios of TAMRA to AuNP. Protease reaction was performed in two methods: one-pot (light gray) and two-step reaction (dark gray). The enzyme (MMP-7) concentration was  $1 \mu\text{g mL}^{-1}$

Fluorescent images also represented the effect of Ni addition to the AuNP-based fluorescence quenching (Fig. 2d). This result strongly indicates that the his-tagged-dye and the carboxy AuNP were tightly associated via nickel coordination, giving rise to a higher fluorescence quenching. The quenching efficiency was calculated using the following equation:  $100 \times (1 - F_{\text{Ni}/\text{AuNP addition}}/F_{\text{Ni}/\text{AuNP-free}})$ , where  $F_{\text{Ni}/\text{AuNP addition}}$  is the fluorescence intensity of the TAMRA peptide in the presence of AuNP and Ni and  $F_{\text{Ni}/\text{AuNP-free}}$  is the fluorescence intensity of the TAMRA peptide in the absence of AuNP and Ni. Particularly, the most significant difference in fluorescence intensity before and after the addition of Ni(II) ion was observed at a 100:1 ratio of TAMRA to AuNP, where the quenching

efficiency is 82.2 %; in other cases, the corresponding quenching efficiencies were 90.0 % for 50:1, 92.6 % for 10:1, 92.8 % for 5:1, and 96.9 % for 1:1. It is worth noting that this quenching efficiency at a 100:1 ratio was much higher than that observed in the direct adsorption of rhodamine dye to the citrate-capped AuNPs [40], supporting the metal affinity interactions of carboxyl AuNPs in the present study.

To gain some insight into the dequenching effect by protease activity, enzyme reaction was attempted with varying ratios of the dye to AuNP in two different ways: a one-pot reaction (all components were mixed at a time) and a two-step reaction (the TAMRA peptide initially reacted with the protease, followed by the addition of other components). MMP-7 was employed as a model protease. As shown in Fig. 3, a strong recovery of fluorescence intensity was observed for 10:1–100:1 quenched solutions by the one-pot enzyme reaction, where the signal intensity increased by 2.8-fold (10:1), 2.4-fold (50:1), and 3.0 fold (100:1) to the quenching state (black and light gray bars in Fig. 3). Compared to that in Fig. 2c, the background intensity in Fig. 3 slightly increased after the quenched solution was subjected to the enzyme reaction condition (2 h at 37 °C). Importantly, the one-pot reaction was found to be much more efficient than the two-step reaction over the differing TAMARA-to-AuNP ratios, indicating that freely moving TAMRA peptide (His<sub>6</sub>) in the initial step of the two-step method is expected to be either not much cleaved by the protease or induce high nonspecific binding to the AuNP after cleavage. It is postulated that the one-pot method enabled histidines to be captured initially by the carboxy AuNP in the presence of Ni<sup>2+</sup>, providing the optimal orientation and structural stability of the peptide–AuNP complex for protease reaction. Unlike the one-pot reaction, when the

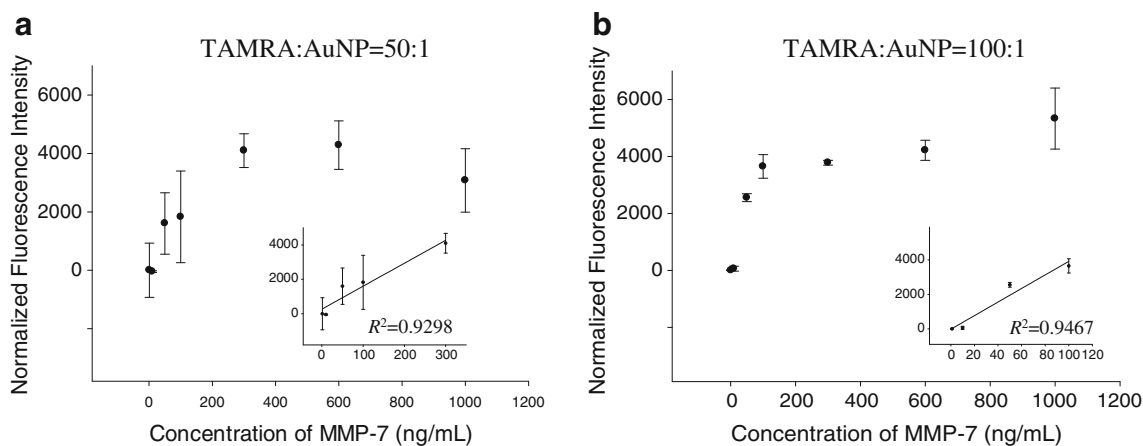


**Fig. 4** Plot of the fluorescence intensity of the TAMRA peptide (His<sub>6</sub>)/Ni(II)/AuNP as a function of MMP-7 concentration ( $1$ – $1,000 \text{ ng mL}^{-1}$ ) at different ratios of TAMRA/AuNP: 50:1 (a) and 100:1 (b). Peak intensities at 580 nm were normalized to the control set without MMP-

7. Error bars represent the standard deviation from two repeated experiments. The inset indicates the linearity between the fluorescence and MMP-7 concentration over the different dynamic ranges

pre-quenched probe was subjected to the same enzyme reaction, no significant signal recovery was observed (data not shown). Despite the similarity in fluorescence recovery, in the case of 100:1, a high binding number and the close packing density of TAMRA peptides on the AuNP surface appear to allow the recovery yield to be slightly improved. These results suggest that the mixing type and timing between the AuNP reactant and enzyme would be very critical for the enzyme reaction, and the all-in-one reaction would be very suited to analyze the protease activity in terms of saving detection time.

To check for enzyme-dependent signal intensity in this system, the protease activity was monitored as a function of the MMP-7 concentration (Fig. 4). When the dequenching intensity was normalized to the control set in the absence of MMP-7, a hyperbolic curve was similarly observed both at a 50:1 (Fig. 4a) and at a 100:1 (Fig. 4b) ratio of the dye to AuNP, ranging from as low as 10 to 1,000 ngmL<sup>-1</sup> in terms of enzyme concentration. Although there was a slight decrease at a high concentration of MMP-7 in the case of a 50:1 ratio of dye to AuNP, the signal recovery showed a plateau after 300 ngmL<sup>-1</sup>, which corresponds to approximately 70 % of the maximum intensity of the TAMRA peptide displayed in Fig. 2a. This reveals that all of the peptides were not likely to be fully cleaved by MMP-7 at a high concentration. Additionally, there was a considerable linearity in the 50:1 ( $R^2=0.9298$  for 10–300 ngmL<sup>-1</sup>) and 100:1 ratios ( $R^2=0.9467$  for 10–100 ngmL<sup>-1</sup>), where the 100:1 ratio condition showed a relatively improved sensitivity and reproducibility over the tested range based on the standard deviation. The detection sensitivity was comparable to those of other assay systems reported previously [22, 41]. Although the dynamic range seems to cover only one order range of the MMP-7 concentration, this result indicates that our developed system is well suited to detect the low concentration range of MMPs. While the AuNP-based colorimetric assay has been well developed [42], such AuNP-based fluorescence detection can offer greater sensitivity in terms of targeting DNA and proteins.

The AuNP-quenched strategy presented in this study has several advantages over the conventional dye-to-quencher system. In addition to the superior quenching effect of AuNPs, the simple and easy fabrication of fluorophore-tethered peptides to the carboxy AuNPs via metal affinity can be achieved without requiring further complicated modifications of the AuNP by multidentate ligands, such as NTA and IDA. This strategy, therefore, enables fluorescent proteins fused to peptides and polyhistidine to be simply conjugated to the AuNP surface. Moreover, since the AuNPs can be generally employed as common quenchers, several fluorophores with different colors could be applied to the AuNPs for a multiplex assay with extremely low background signal.

## Conclusion

In conclusion, we demonstrated the simple assay of protease activity using the AuNP-based fluorescence quenching system via metal affinity. Simple and rapid association between the carboxy groups of AuNPs and the hexahistidine regions of the dye-tethered peptides was observed in the presence of Ni(II) ions, leading to notable fluorescence quenching over varying molar ratios (100:1–1:1) of the dye to AuNP. When MMP-7 was added to the AuNP–dye solution, significant fluorescence dequenching was found, especially at 10:1–100:1 dye-to-AuNP molar ratios, where the detection limit was as low as 10 ngmL<sup>-1</sup>. By combining fluorophores with different colors, this developed system will have great potential to study the protease activity with low background and high sensitivity.

**Acknowledgment** This work was supported by the Basic Science Research Program (2012-0008222), the Bio-Signal Analysis Technology Innovation Program (2012-0006053), and the Nano Material Technology Development Program (2012035286) through the National Research Foundation of Korea (NRF) funded by the Ministry of Education, Science and Technology.

**Open Access** This article is distributed under the terms of the Creative Commons Attribution License which permits any use, distribution and reproduction in any medium, provided the original author(s) and source are credited.

## References

- Dubertret B, Calame M, Libchaber AJ (2001) Single-mismatch detection using gold-quenched fluorescent oligonucleotides. *Nat Biotechnol* 19(7):680–681
- Dulkeith E, Morteani AC, Niedereichholz T, Klar TA, Feldmann J, Levi SA, van Veggel FCJM, Reinhoudt DN, Moller M, Gittins DI (2002) Fluorescence quenching of dye molecules near gold nanoparticles: radiative and nonradiative effects. *Phys Rev Lett* 89(20):203002
- Maxwell DJ, Taylor JR, Nie SM (2002) Self-assembled nanoparticle probes for recognition and detection of biomolecules. *J Am Chem Soc* 124(32):9606–9612
- Rosi NL, Mirkin CA (2005) Nanostructures in biodiagnostics. *Chem Rev* 105(4):1547–1562
- Bunz UHF, Rotello VM (2010) Gold nanoparticle–fluorophore complexes: sensitive and discerning “noses” for biosystems sensing. *Angew Chem Int Edit* 49(19):3268–3279
- Acuna GP, Bucher M, Stein IH, Steinhauer C, Kuzyk A, Holzmeister P, Schreiber R, Moroz A, Stefani FD, Liedl T, Simmel FC, Tinnefeld P (2012) Distance dependence of single-fluorophore quenching by gold nanoparticles studied on DNA origami. *ACS Nano* 6(4):3189–3195
- Sen T, Sadhu S, Patra A (2007) Surface energy transfer from rhodamine 6G to gold nanoparticles: a spectroscopic ruler. *Appl Phys Lett* 91(4):2762283
- Yun CS, Javier A, Jennings T, Fisher M, Hira S, Peterson S, Hopkins B, Reich NO, Strouse GF (2005) Nanometal surface

- energy transfer in optical rulers, breaking the FRET barrier. *J Am Chem Soc* 127(9):3115–3119
9. Jennings TL, Singh MP, Strouse GF (2006) Fluorescent lifetime quenching near  $d=1.5$  nm gold nanoparticles: probing NSET validity. *J Am Chem Soc* 128(16):5462–5467
  10. Kim JH, Estabrook RA, Braun G, Lee BR, Reich NO (2007) Specific and sensitive detection of nucleic acids and RNases using gold nanoparticle–RNA–fluorescent dye conjugates. *Chem Commun* 42:4342–4344
  11. Obliosca JM, Wang PC, Tseng FG (2012) Probing quenched dye fluorescence of Cy3–DNA–Au-nanoparticle hybrid conjugates using solution and array platforms. *J Colloid Interface Sci* 371:34–41
  12. Wang WJ, Chen CL, Qian MX, Zhao XS (2008) Aptamer biosensor for protein detection using gold nanoparticles. *Anal Biochem* 373(2):213–219
  13. Kim YP, Oh YH, Kim HS (2008) Protein kinase assay on peptide-conjugated gold nanoparticles. *Biosens Bioelectron* 23(7):980–986
  14. Mayilo S, Kloster MA, Wunderlich M, Lutich A, Klar TA, Nichtl A, Kurzinger K, Stefani FD, Feldmann J (2009) Long-range fluorescence quenching by gold nanoparticles in a sandwich immunoassay for cardiac troponin T. *Nano Lett* 9(12):4558–4563
  15. Guirgis BSS, Cunha CSE, Gomes I, Cavadas M, Silva I, Doria G, Blatch GL, Baptista PV, Pereira E, Azzazy HME, Mota MM, Prudencio M, Franco R (2012) Gold nanoparticle-based fluorescence immunoassay for malaria antigen detection. *Anal Bioanal Chem* 402(3):1019–1027
  16. Hu PP, Chen LQ, Liu C, Zhen SJ, Xiao SJ, Peng L, Li YF, Huang CZ (2010) Ultra-sensitive detection of prion protein with a long range resonance energy transfer strategy. *Chem Commun* 46(43):8285–8287
  17. Kim GB, Kim YP (2012) Analysis of protease activity using quantum dots and resonance energy transfer. *Theranostics* 2(2):127–138
  18. Lee H, Lee K, Kim IK, Park TG (2008) Synthesis, characterization, and in vivo diagnostic applications of hyaluronic acid immobilized gold nanoprobe. *Biomaterials* 29(35):4709–4718
  19. Chen WY, Lan GY, Chang HT (2011) Use of fluorescent DNA-templated gold/silver nanoclusters for the detection of sulfide ions. *Anal Chem* 83(24):9450–9455
  20. Jin LH, Shang L, Guo SJ, Fang YX, Wen D, Wang L, Yin JY, Dong SJ (2011) Biomolecule-stabilized Au nanoclusters as a fluorescence probe for sensitive detection of glucose. *Biosens Bioelectron* 26(5):1965–1969
  21. Huang Y, Zhao SL, Liang H, Chen ZF, Liu YM (2011) Multiplex detection of endonucleases by using a multicolor gold nanobeacon. *Chem-Eur J* 17(26):7313–7319
  22. Kim YP, Oh YH, Oh E, Ko S, Han MK, Kim HS (2008) Energy transfer-based multiplexed assay of proteases by using gold nanoparticle and quantum dot conjugates on a surface. *Anal Chem* 80(12):4634–4641
  23. Swierczewska M, Lee S, Chen XY (2011) The design and application of fluorophore-gold nanoparticle activatable probes. *Phys Chem Chem Phys* 13(21):9929–9941
  24. Welser K, Adsley R, Moore BM, Chan WC, Aylott JW (2011) Protease sensing with nanoparticle based platforms. *Analyst* 136(1):29–41
  25. Turk B (2006) Targeting proteases: successes, failures and future prospects. *Nat Rev Drug Discov* 5(9):785–799
  26. Lowe SB, Dick JAG, Cohen BE, Stevens MM (2012) Multiplex sensing of protease and kinase enzyme activity via orthogonal coupling of quantum dot peptide conjugates. *ACS Nano* 6(1):851–857
  27. Mu CJ, LaVan DA, Langer RS, Zetter BR (2010) Self-assembled gold nanoparticle molecular probes for detecting proteolytic activity in vivo. *ACS Nano* 4(3):1511–1520
  28. Free P, Shaw CP, Levy R (2009) PEGylation modulates the interfacial kinetics of proteases on peptide-capped gold nanoparticles. *Chem Commun* 33:5009–5011
  29. Lee S, Cha EJ, Park K, Lee SY, Hong JK, Sun IC, Kim SY, Choi K, Kwon IC, Kim K, Ahn CH (2008) A near-infrared-fluorescence-quenched gold-nanoparticle imaging probe for in vivo drug screening and protease activity determination. *Angew Chem Int Edit* 47(15):2804–2807
  30. Hainfeld JF, Liu WQ, Halsey CMR, Freimuth P, Powell RD (1999) Ni–NTA–gold clusters target his-tagged proteins. *J Struct Biol* 127(2):185–198
  31. Swartz JD, Gulka CP, Haselton FR, Wright DW (2011) Development of a histidine-targeted spectrophotometric sensor using Ni(II)NTA-functionalized Au and Ag nanoparticles. *Langmuir* 27(24):15330–15339
  32. Hochuli E, Bannwarth W, Dobeli H, Gentz R, Stuber D (1988) Genetic approach to facilitate purification of recombinant proteins with a novel metal chelate adsorbent. *Nat Biotechnol* 6(11):1321–1325
  33. Yao HQ, Zhang Y, Xiao F, Xia ZY, Rao JH (2007) Quantum dot/bioluminescence resonance energy transfer based highly sensitive detection of proteases. *Angew Chem Int Edit* 46(23):4346–4349
  34. Sternlicht MD, Werb Z (2001) How matrix metalloproteinases regulate cell behavior. *Annu Rev Cell Dev Biol* 17:463–516
  35. Egeblad M, Werb Z (2002) New functions for the matrix metalloproteinases in cancer progression. *Nat Rev Cancer* 2(3):161–174
  36. Page-McCaw A, Ewald AJ, Werb Z (2007) Matrix metalloproteinases and the regulation of tissue remodelling. *Nat Rev Mol Cell Biol* 8(3):221–233
  37. Cumberland SL, Strouse GF (2002) Analysis of the nature of oxyanion adsorption on gold nanomaterial surfaces. *Langmuir* 18(1):269–276
  38. Lewis DJ, Day TM, MacPherson JV, Pikramenou Z (2006) Luminescent nanobeads: attachment of surface reactive Eu(III) complexes to gold nanoparticles. *Chem Commun* 13:1433–1435
  39. Block H, Maertens B, Spriestersbach A, Brinker N, Kubicek J, Fabis R, Labahn J, Schafer F (2009) Immobilized-metal affinity chromatography (IMAC): a review. *Method Enzymol* 463:439–473
  40. Stobiecka M, Hepel M (2011) Multimodal coupling of optical transitions and plasmonic oscillations in rhodamine B modified gold nanoparticles. *Phys Chem Chem Phys* 13(3):1131–1139
  41. Kim YP, Oh YH, Oh E, Kim HS (2007) Chip-based protease assay using fluorescence resonance energy transfer between quantum dots and fluorophores. *Biochip J* 1(4):228–233
  42. Wang LH, Zhang J, Wang X, Huang Q, Pan D, Song SP, Fan CH (2008) Gold nanoparticle-based optical probes for target-responsive DNA structures. *Gold Bull* 41(1):37–41